Heavy Flavour Hadroproduction

D. Houseman*
High Energy Physics, University College, London

6 June 2008

Abstract

The total cross section for heavy quark hadroproduction receives large corrections from NLO and higher-order terms in the limit of either a) the parton center-of-mass energy near threshold or b) the parton center-of-mass energy much larger than threshold. This research is directed towards understanding the resummation of both types of corrections and incorporating both types of correction into a single framework.

Introduction

Heavy flavour physics provides an excellent testing ground for perturbative QCD, due to the smallness of the coupling constant α_S at the heavy quark mass M. The LHC will rapidly accumulate very high statistics of $t\bar{t}$ and $b\bar{b}$ pairs (Figure 1). Comparison with precise theoretical predictions for heavy quark production rates may reveal signals for new physics, as heavy flavours are copious sources of leptons [13]. However, this will require further progress in precisely determining corrections to the heavy quark cross sections. Additionally, some recent attention has been directed towards the suitability of the top-pair total cross section as a 'standard candle' process for the LHC [12] (that is, a process which is known so precisely that it may be used to determine beam luminosity), though this will require further improvements constraining both theoretical and experimental uncertainties. This paper will consider some aspects of the theoretical uncertainties associated with heavy quark production at the LHC.

*email: houseman@hep.ucl.ac.uk

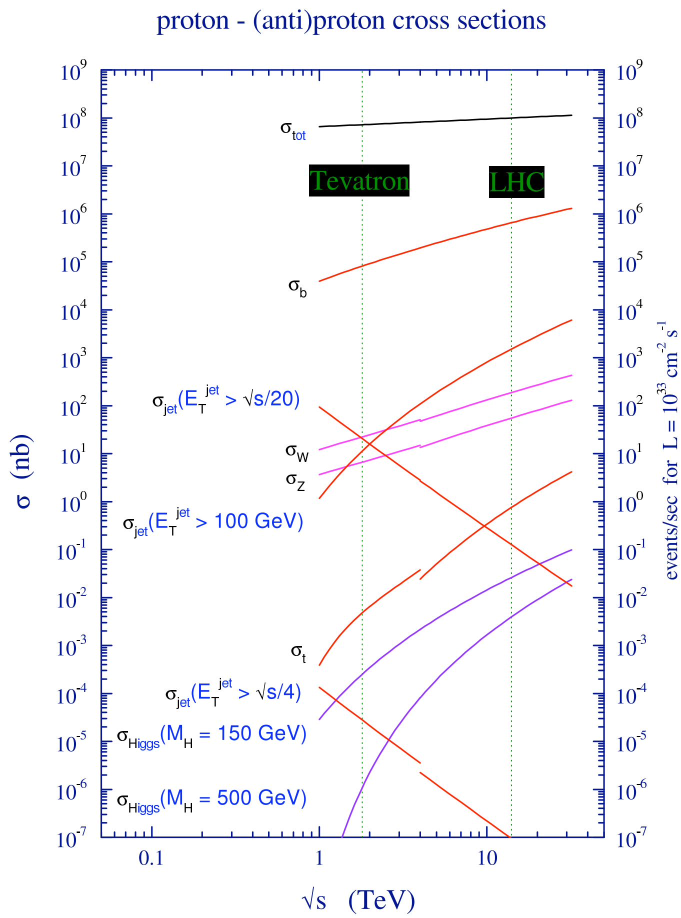

Figure 1: Standard model cross sections at the Tevatron and LHC. From Campbell *et al* [4].

Leading Order (LO) Heavy Flavour Production

The total hadronic cross section is given by ([6], Ch. 10)

$$\sigma(P_1, P_2) = \sum_{i,j} \int dx_1\, dx_2\, f_i(x_1, \mu^2) f_j(x_2, \mu^2)\, \hat{\sigma}_{ij}(s, m^2 \mu^2) \tag{1}$$

where $f_i(x_1, \mu^2)$ is the parton distribution function for the ith parton species, evaluated at renormalisation scale μ. $\hat{\sigma}_{ij}$ is called the partonic cross section. The leading-order contributions to for production of a heavy quark Q are quark-antiquark annihilation (Fig 2a) and gluon fusion (Fig 2b), and there is no gluon-quark contribution at this order. At the LHC, $b\bar{b}$ quark pairs are produced at low Bjorken-x, and owing to the large gluon densities at low x, gluon fusion will be the dominant contribution to the cross section. On the other hand, $t\bar{t}$ quark pairs are produced nearer to threshold (and hence at fairly large x), and the larger valence quark densities at high x drive a larger contribution from $q\bar{q}$ annihilation.

The matrix elements squared for the leading order diagrams are computed using the Feynman rules and summing (averaging) over initial (final) colours and spins, and are shown in Table 1. An abbreviated notation for the ratios of scalar products has been used:

$$\tau_1 = \frac{2p_1 \cdot p_3}{\hat{s}}, \qquad \tau_2 = \frac{2p_2 \cdot p_3}{\hat{s}}, \qquad \hat{s} = (p_1 + p_2)^2, \qquad \rho = \frac{4M^2}{\hat{s}}. \tag{2}$$

ρ is the (square) ratio of $2M$, the energy required to create the $Q\bar{Q}$ pair, to the invariant mass $\hat{s}$ of the incoming partons. Consequently, $\rho \sim 1$ corresponds to a $Q\bar{Q}$ pair produced near threshold, and $\rho \to 0$ describes the high energy limit. The minimum value for ρ depends on the ratio of the heavy quark mass to the collider energy, though in practice $\hat{s}$ is less than about 10% of the collider energy S since parton densities above $x \sim 0.3$ are small.

The partonic cross section is obtained from the matrix element using

$$d\hat{\sigma}_{ij} = \frac{1}{2\hat{s}} \frac{d^3p_3}{(2\pi)^3 2E_3} \frac{d^3p_4}{(2\pi)^3 2E_4} (2\pi)^4\, \delta^4(p_1 + p_2 - p_3 - p_4) \overline{\sum} |M_{ij}|^2. \tag{3}$$

The integration can be performed explicitly and the leading order contribu-

Table 1: Matrix elements squared at leading order.

	$\overline{\sum}\lvert M_{ij}\rvert^2/g^4$
$q\bar{q} \to Q\bar{Q}$	$\frac{4}{9}\left(\tau_1^2+\tau_2^2+\frac{\rho}{2}\right)$
$gg \to Q\bar{Q}$	$\left(\frac{1}{6\tau_1\tau_2}-\frac{3}{8}\right)\left(\tau_1^2+\tau_2^2+\rho-\frac{\rho^2}{4\tau_1\tau_2}\right)$

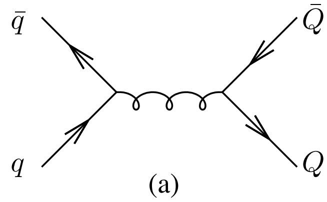

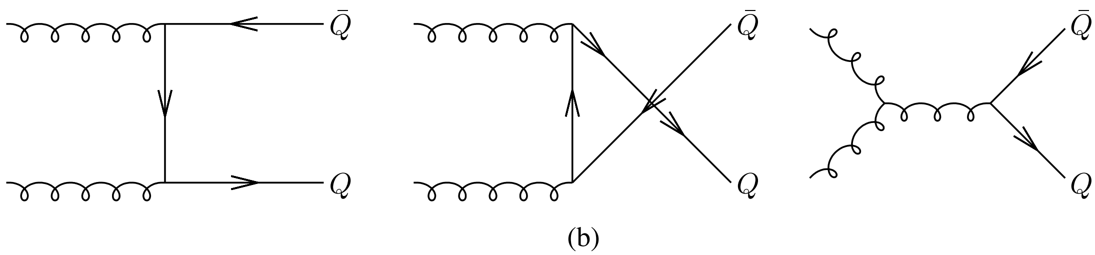

Figure 2: a. $q\bar{q} \to Q\bar{Q}$. b. $g\bar{g} \to Q\bar{Q}$ in t, u, s channels.

tions to the partonic cross sections are [6]

$$\begin{aligned}
F_{q\bar{q}}^{(0)}(\rho) &= \frac{\pi\beta\rho}{27}(2+\rho) \\
F_{gg}^{(0)}(\rho) &= \frac{\pi\beta\rho}{192}\left(\frac{1}{\beta}(\rho^2+16\rho+16)\ln\left(\frac{1+\beta}{1-\beta}\right)-28-31\rho\right) \\
F_{gq}^{(0)}(\rho) &= F_{g\bar{q}}^{(0)}(\rho) = 0
\end{aligned} \tag{4}$$

where the partonic cross sections are related to the with dimensionless functions F_{ij} by

$$d\hat{\sigma}_{ij} = \frac{\alpha_S^2(\mu^2)}{m^2}F_{ij}\left(\rho, \mu^2/m^2\right) \tag{5}$$

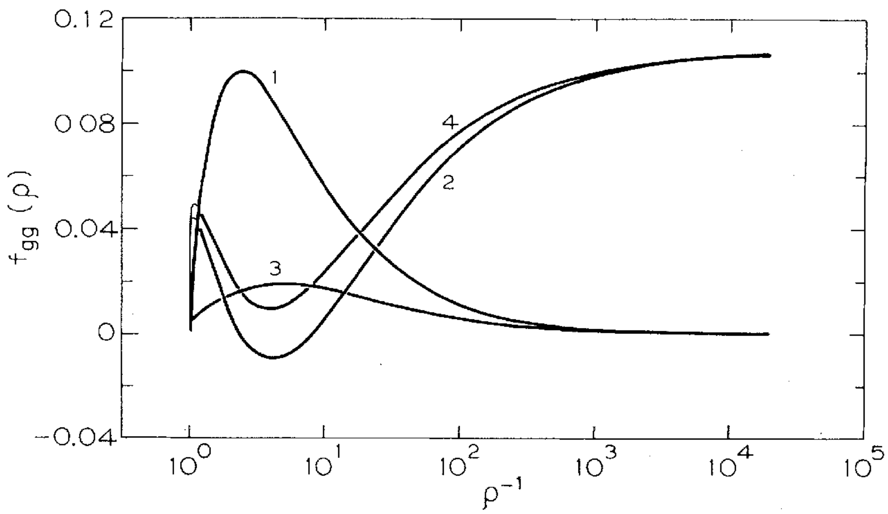

Figure 3: Gluon-gluon cross section $\hat{\sigma}_{gg}$. (1) LO contribution. (2-4) NLO contributions. (From Beenakker *et al* [3].)

and $\beta = \sqrt{1-\rho}$ is the velocity of the $Q\bar{Q}$ pair. The LO contribution to the gluon-gluon cross section $\hat{\sigma}_{gg}$ is the curve labelled (1) in Fig 3. For $t\bar{t}$ pairs at the LHC ($S = 14$TeV), the kinematic range of ρ^{-1} is from 1 to about 160, so only the left hand side of of Fig 3 is relevant. At the Tevatron ($S = 2$TeV), top pairs are restricted to an even smaller kinematic range in the threshold region. For $b\bar{b}$ pairs at the LHC, ρ^{-1} ranges from 1 up to about 2×10^5, so the full range of the plot is relevant in this case.

Next-to-leading Order (NLO) Heavy Flavour Production

The order α_S^3 corrections to the total partonic cross-section were computed numerically by Nason et al. [13] and analytically Beenakker et al. [3]. The curves (2-4) in Figure 3 are different NLO contributions to $\hat{\sigma}_{gg}$. The figure shows that NLO processes provide large corrections over the whole kinematic range. Indeed, NLO contributions dominate in both the threshold region $\rho \sim 1$ and in the high-energy limit $\rho \gg 1$, since the LO contribution (the curve (1) in Figure 3) vanishes in either of these limits. This is a striking illustration of the importance of higher-order corrections to theoretical predictions, and becomes evident in predictions for the total $Q\bar{Q}$ cross section: the NLO prediction for $b\bar{b}$ production at the LHC is larger than the LO prediction by more than 100%.

Corrections in the threshold region $\rho \sim 1$ are called threshold corrections, may be handled using the technique of threshold resummation [9]. Corrections in the high-energy limit $\rho \gg 1$ are analysed using high-energy (low-x) resummation [2]. For top quark production at the LHC or Tevatron, threshold corrections provide a large contribution to the cross section, but high-energy resummation corrections can be neglected. For bottom quark production at the LHC, both threshold corrections and high-energy corrections must be included.

Prospects for NNLO Heavy Flavour Production

Only a few processes have been computed exactly to NNLO. The first examples were $W^{\pm}$ and Z production; these processes are more amenable to analysis because at tree level they couple only to quark-antiquark external legs and not to gluons. Vogt *et al* [14] have recently computed parton splitting functions to NNLO. Higgs production has been computed to NNLO under the simplifying approximation that the Higgs mass is much less than twice the top mass [1]. In comparison to these processes, heavy flavour hadroproduction faces significant challenges owing to the gluon legs, which are analytically much more demanding than quark/antiquark legs. As a result, it is likely to be at least several years before NNLO analysis of heavy flavour hadroproduction is completed.

However, significant progress towards a NNLO result can be made by extending NLO results in various simplifying limits. Figure 4 shows the result of Vogt *et al* [14] for the NNLO parton splitting function $P_{ps}(x)$ (a mathematical expression one-and-a-half pages long!), compared to earlier estimates based on different extensions of NLO results. The agreement is excellent over the full range of x. This is encouraging for the problem of heavy flavour production, because in the absence of exact NNLO results similar analyses extending NLO results may also be able to give good results. The immediate aim of my PhD is to understand the methods of analysis by which NLO results for heavy flavour hadroproduction might be improved. The remainder of this paper will give a brief introduction to some of the

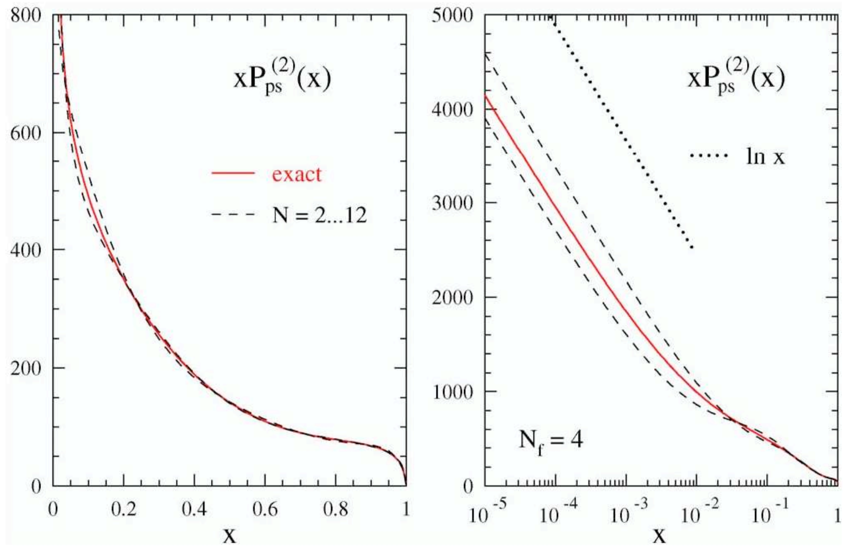

Figure 4: *(a)* The NNLO pure singlet splitting function (solid line) compared to earlier estimates (dashed line) based on NLO arguments. *(b)* The same as *(a)*, at low x. (From Vogt *et al.* [14].)

main tools that are currently employed in the literature.

BFKL and High-Energy Resummation

Heavy flavour hadroproduction is the production of heavy quark pairs in hadron collisions (Figure 5). A recent result by Ball & Ellis [2] resums the leading logarithmic terms at high energy to provide estimates on the high energy corrections. The analysis is closely related to the BFKL equation, which will be described in this section.

Asymptotic freedom of QCD at high energy S means that the coupling constant α_S is small at the scale of the quark mass M. However, successive terms in the order-by-order expansion generally involve coefficients of the form $\ln^m S/M^2$ [5]; the *leading logarithmic terms* at successive orders in α_S involve successive powers of $\alpha_S \ln S/M^2$. In the high energy limit $S \gg M^2$,

$$\alpha_S \ln S/M^2 \sim 1 \tag{6}$$

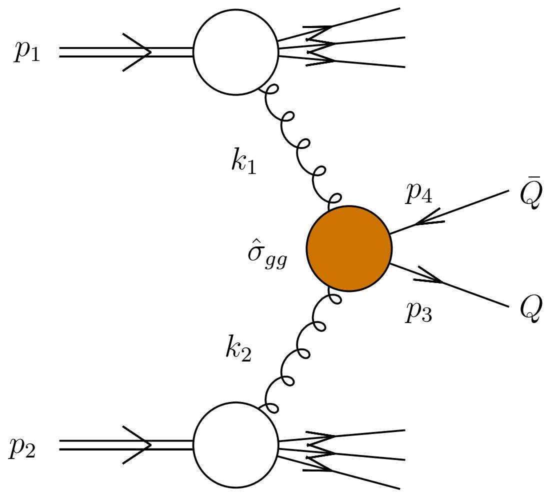

Figure 5: $Q\bar{Q}$ hadroproduction. The shaded circle represents the three gg-processes in Figure 2b.

and NLO, NNLO and higher order terms of the perturbative series may therefore contribute large corrections to the amplitude. This is evident from the discussion of bottom quark hadroproduction, where the NLO prediction for the total cross section is larger than the LO prediction by 100%.

However, in the limit of high energy and small x, it is precisely the leading logarithmic terms which provide the dominant contribution to the amplitude at each order of the pertubative series. The Balitsky-Fadin-Kuraev-Lipatov (BFKL) [10] equation in its simplest form accounts for the leading logarithmic terms to all orders (a process referred to as *resummation*), and neglects all terms of subleading order in $\ln S/M^2$. The schematic diagram in Figure 6 illustrates all contributions to an amplitude as coefficients of $\alpha_S^m \ \ln^n S/M^2$. The leading logarithmic (LL) terms which are resummed in the BFKL equation are indicated. Next-to-leading logarithmic (NLL) terms, which are the major subleading contribution to the amplitude, are also indicated.

In the centre-of-mass frame of the incoming protons,

$$p_1 = \tfrac{1}{2}\sqrt{S}(1,0,0,1), \qquad p_2 = \tfrac{1}{2}\sqrt{S}(1,0,0,-1). \tag{7}$$

where in the high energy limit the proton mass can be neglected. Following e.g., [8], p.29, the Sudakov parametrisation for the momenta of the exchanged

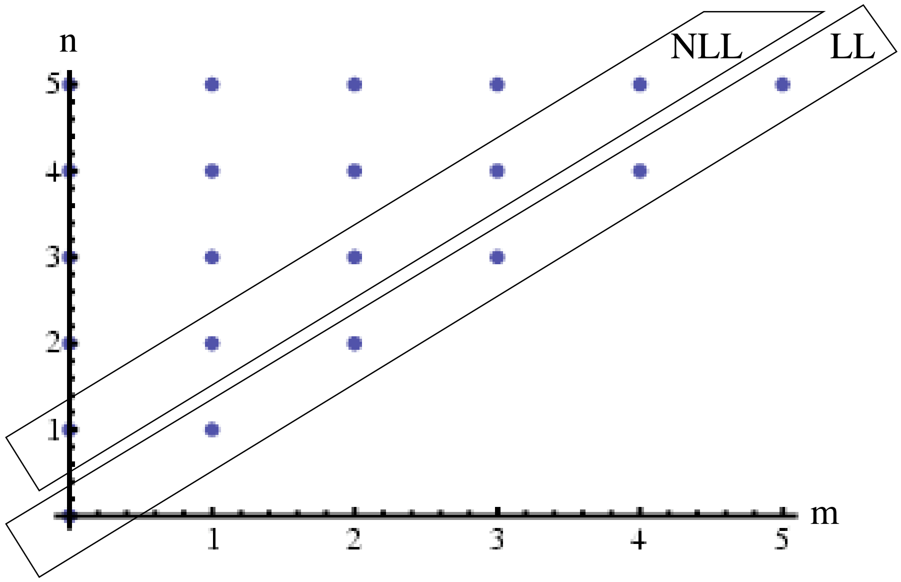

Figure 6: QCD contributions to an amplitude are of the form $\alpha_S^m \ \ln^n S/M^2$. Leading logarithms (LL) and next-to-leading logarithms (NLL) are indicated.

gluon partons k_1, k_2 is

$$k_1 = \bar{z}_1 p_1 + z_1 p_2 + k_{1\perp}, \qquad k_2 = \bar{z}_2 p_1 + z_2 p_2 + k_{2\perp}. \tag{8}$$

The Sudakov parametrisation separates the parton momenta into components collinear with the proton momenta p_1, p_2, and a transverse component $k_{1,2\perp}$ perpendicular to p_1 and p_2. $k_{1,2\perp}$ are conventionally denoted by 2-vectors $\mathbf{k_1}$, $\mathbf{k_2}$. $z_1, z_2, \bar{z}_1$ and $\bar{z}_2$ are called the Sudakov parameters or longitudinal momentum fractions. They have Lorentz invariant expressions

$$z_1 = \frac{2p_1k_1}{S}, \qquad z_2 = \frac{2p_1k_2}{S}, \qquad \bar{z}_1 = \frac{2p_2k_1}{S}, \qquad \bar{z}_2 = \frac{2p_2k_2}{S} \tag{9}$$

This analysis will focus on the case where the heavy quark pair is produced in the central rapidity region, for which the parameters $\bar{z}_1, z_2$ are small. In this regime, $s \gg t$. At high energy, the cross section is dominated by t-channel gluon exchange, because multiple s-channel gluon processes are suppressed by powers of $\alpha_S(M^2)$ (they are 'higher twist corrections'). This

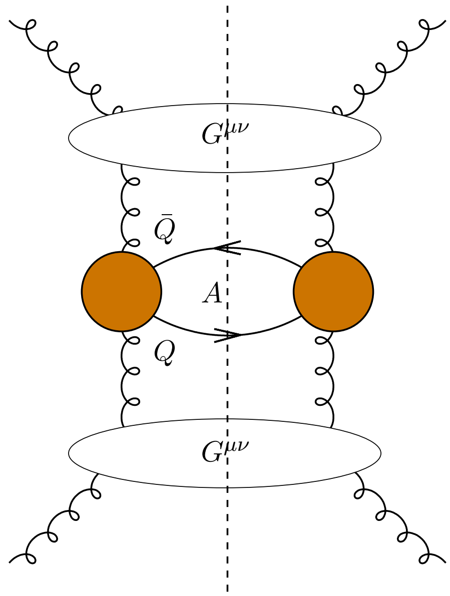

Figure 7: Factorisation of the partonic cross section σ.

leads to the factorisation [5]

$$\sigma = \frac{1}{2S}\int\frac{d^4k_1}{(2\pi)^4}\int\frac{d^4k_2}{(2\pi)^4}A_{\mu_1\nu_1,\mu_2\nu_2}(k_1,k_2)G^{\mu_1\nu_1}(p_1,k_1)G^{\mu_2\nu_2}(p_2,k_2) \tag{10}$$

where $A_{\mu\nu}$ is the absorptive amplitude for two off-shell gluons k_1, k_2 and $G^{\mu\nu}$ is the gluon-gluon amplitude. This factorisation is illustrated in Fig 7. Fig 7 is called a 'cut' diagram and uses the optical theorem to evaluate the total inclusive cross section.

$\bar{z}_1$ and z_2 are small, and it can be shown that this leads to the simplification of (10) to a convolution in $\bar{z}_1$ and z_2,

$$\begin{aligned}\sigma(\rho) = \frac{1}{4M^2}\int d^2\mathbf{k}_1\int\frac{d\bar{z}_1}{\bar{z}_1}\int d^2\mathbf{k}_2\int\frac{dz_2}{z_2}\\ \mathcal{F}(\bar{z}_1,\mathbf{k}_1)\ \mathcal{F}(z_2,\mathbf{k}_2)\hat{\sigma}_{gg}(\rho/\bar{z}_1z_2,\mathbf{k}_1/M,\mathbf{k}_2/M).\end{aligned} \tag{11}$$

$\mathcal{F}(z,k;Q_0^2)$ is called the unintegrated gluon structure function, and it obeys the Balitsky-Fadin-Kuraev-Lipatov (BFKL) evolution equation [10].

$$\mathcal{F}(x,\mathbf{k}) = \frac{1}{\pi}\delta(1-x)\delta(\mathbf{k}^2 - Q_0^2) + \bar{\alpha}_S \int \frac{d^2\mathbf{q}}{\pi \mathbf{q}^2} \int \frac{dz}{z} \left(\mathcal{F}\left(\frac{x}{z}, \mathbf{k}+\mathbf{q}\right) - \Theta(k-q)\mathcal{F}\left(\frac{x}{z}, \mathbf{k}+\mathbf{q}\right)\right) \tag{12}$$

where Q_0^2 is the virtuality of the gluon emitted directly from the proton, and is therefore low (of the order of Λ_{QCD}). $\mathbf{k}^2$ is the virtuality of the gluon at the top of the ladder (the gluon which is absorbed at the heavy quark). The first term of (12) (the delta functions) correspond to the lowest order process, where the gluon is emitted and absorbed without radiating. The second term of (12) (the integral) gives the effect of the initial gluon at Q_0^2 radiating further gluons.

The BFKL equation (12) determines $\mathcal{F}$, and an explicit solution can be obtained by using a Mellin transform in the variable x. The Mellin transform of $\mathcal{F}(x,\mathbf{k})$ is defined to be

$$\mathcal{F}_N(\mathbf{k}) = \int_0^1 dx\; x^{N-1}\mathcal{F}(x,\mathbf{k}) \tag{13}$$

for all $N \geq 0$. Applying the Mellin transform to (12) 'undoes' the z-integral in a similar fashion to how the Laplace transform undoes a convolution integral. Averaging over the angular dependence of $\mathbf{q}$, and noting that the Mellin transform of $\delta(1-x)$ is identically 1, (12) can be written in the form.

$$\mathcal{F}_N(\mathbf{k}^2) = \frac{1}{\pi}\delta(\mathbf{k}^2 - Q_0^2) + \frac{\bar{\alpha}_S}{N}\int_0^1 \frac{d\lambda}{1-\lambda}\left(\mathcal{F}_N(\lambda\mathbf{k}^2) + \frac{1}{\lambda}\mathcal{F}_N(\frac{\mathbf{k}^2}{\lambda}) - 2\mathcal{F}_N(\mathbf{k}^2)\right) \tag{14}$$

Eigenfunctions of the integral term on the right-hand side of (14) are

$$\mathcal{F}_N(\mathbf{k}^2) = (\mathbf{k}^2)^{\gamma-1} \tag{15}$$

for all complex γ; the corresponding eigenvalues are

$$\chi(\gamma) = 2\psi(1) - \psi(\gamma) - \psi(1-\gamma) \tag{16}$$

(the Lipatov characteristic function). A plot of $\chi(\gamma)$ is shown in Figure 8.

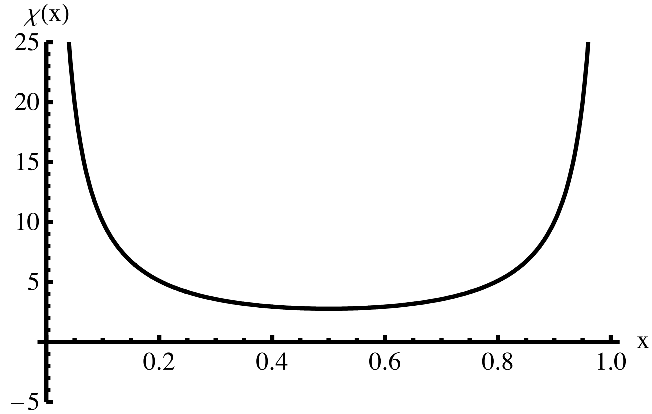

Figure 8: The Lipatov characteristic function.

The eigenfunctions (15) form a complete set for $\gamma = 1/2 + it$, with t real, and it is possible to solve (14) and obtain

$$\mathcal{F}_N(\mathbf{k}^2) = \frac{1}{\pi \mathbf{k}^2} \int_{1/2-i\infty}^{1/2+i\infty} \frac{d\gamma}{2\pi i} \left(1 - \frac{\bar{\alpha}_S}{N}\chi(\gamma)\right)^{-1} \left(\frac{\mathbf{k}^2}{Q_0^2}\right)^{\gamma} \tag{17}$$

In (17), the denominator of the integrand vanishes at points γ_N in the complex plane for which

$$\chi(\gamma) = \frac{N}{\bar{\alpha}_S}. \tag{18}$$

The solution γ_N of (18) becomes a simple pole for the contour integral in the inverse Mellin transformation (17). Because it appears as the exponent of $\mathbf{k}^2$ in the gluon structure function $\mathcal{F}_N$ in (17), γ_N is called the *anomalous dimension*. For $N \gg \bar{\alpha_S}$, perturbative solution of (18) gives

$$\gamma_N = \frac{\bar{\alpha}_S}{N} + 2\zeta(3)\left(\frac{\bar{\alpha}_S}{N}\right)^4 + \ldots \tag{19}$$

where ζ is the Riemann zeta-function. γ_N may not exceed 0.5 (this corresponds to the minimum value of the Lipatov characteristic function in Fig 8); it becomes a 'pomeron' beyond this point.

Inserting γ_N into (17) provides the dominant contribution to the unintegrated structure function $\mathcal{F}$, and includes all the high-energy leading logarithms. Ball & Ellis [2] convolve this with the (off-shell) heavy-quark hard cross section $\hat{\sigma}_{gg}$ to provide the resummed heavy quark hadroproduction cross section. In the the near future, I intend to investigate their analysis further.

Threshold corrections

Threshold large logarithms are of the form $\alpha_S^3 \ln(s - 4m_b^2)$ and diverge in the limit that $(s - 4m_b^2)$ is small, that is, when s is just above threshold for production of the $b\bar{b}$ pair. For this reason, these terms dominate the cross section near threshold and can be used to estimate the total cross section in this regime. Kidonakis *et al* [9] have developed a method of resumming these logarithms, which is perhaps analogous to the resummation of high-energy leading logarithms discussed in the previous section. This is also a topic I intend to study soon.

Outlook

High-energy corrections, following Ball & Ellis, and threshold corrections, following Kidonakis *et al*, provide estimates on the major corrections to the heavy quark inclusive cross section at both kinematic limits accessible at the LHC. It may be possible to incorporate both sets of results into a single framework, to provide estimates on corrections over the full kinematic range. This is an approach that in the past has been successful in the context of parton splitting functions.

Acknowledgments

I wish to thank my supervisor, R. Thorne, for his patient supervision and guidance during the first year of my doctorate.

References

[1] C. Anastasiou and K. Melnikov. *Nucl. Phys*, B646:220, 2002.

[2] R. D. Ball and R. K. Ellis. *JHEP*, 05:053, 2001.

[3] W. Beenakker, H. Kuijf, W. L. van Neerven, and J. Smith. *Phys. Rev.*, D40:54–82, 1989.

[4] J. M. Campbell, J. W. Huston, and W. J. Stirling. *Rep. Prog. Phys.*, 70:89, 2007.

[5] S. Catani, M. Ciafaloni, and F. Hautmann. *Nucl. Phys.*, B366:135, 1991.

[6] R. K. Ellis, W. J. Stirling, and B. R. Webber. *QCD and Collider Physics.* Cambridge, 1996.

[7] V. S. Fadin, E. A. Kuraev, and L. N. Lipatov. *Phys. Lett.*, 60B:50, 1975.

[8] J. R. Forshaw and D. A. Ross. *Quantum Chromodynamics and the Pomeron.* Cambridge Lect. Notes Phys., 1997.

[9] N. Kidonakis, E. Laenen, S. Moch, and R. Vogt. *Phys. Rev.*, D64:114001, 2001.

[10] E. A. Kuraev, L. N. Lipatov, and V. S. Fadin. *Sov. Phys. JETP*, 45:199–204, 1977.

[11] E. Laenen, J. Smith, and W. L. van Neerven. *Nucl. Phys.*, B369:543–599, 1992.

[12] M. Mangano. *Talk given at 'HERA and the LHC' Conference, CERN*, 2008.

[13] P. Nason, S. Dawson, and R. K. Ellis. *Nucl. Phys.*, B303:607, 1988.

[14] A. Vogt, S. Moch, and J. A. M. Vermaseren. *Nucl. Phys.*, B691:129, 2004.

[15] C. D. White. *Heavy Flavour Production at Small-x.* PhD Thesis, Cambridge, 2006.